Supplement of Earth Surf. Dynam., 13, 647–663, 2025
https://doi.org/10.5194/esurf-13-647-2025-supplement


Earth Surface Dynamics
Open Access
EGU

*Supplement of*

# Localised geomorphic response to channel-spanning leaky wooden dams

**Joshua M. Wolstenholme et al.**

*Correspondence to:* Joshua M. Wolstenholme (j.m.wolstenholme@lboro.ac.uk)

**S1. Flow frequency analysis**

In lieu of long term flow data available for Staindale Beck, analysis was performed on the annual maximum series of two Environment Agency gauges, L2725 of Thornton le Dale, of which Staindale Beck is a tributary, and F25110 of a catchment adjacent to the study area (Crown copyright (2023). Both gauges have 15-minute resolution level measurements, and F25110 has discharge available but there is low confidence when stage is >0.4 m due to the unconstrained channel (Hydrology NE Environment Agency, 2024). Flow frequency analysis was performed by 1) fitting the General Extreme Value Distribution to the annual maximum series of L2725 and F25110; 2) comparing the median normalised percentage exceedance curves for the study time period; and 3) performing cross-correlation comparisons between recorded level data at the most upstream logger (herein L590).

*Table S1: Monitoring gauges used for analysis. †Environment Agency, *this study. Grid references shown are in British National Grid (EPSG:27700).*

| Gauge ID | Location | Upstream area | Grid Reference | Start of record | Record length (years) |
|---|---|---|---|---|---|
| L2725† | Thornton Beck at Thornton le Dale | 33.3 $km^2$ | SE 83681 83418 | 19/02/08 | 16 |
| F25110† | Levisham Beck at Levisham Mill | 12.0 $km^2$ | SE 83532 90119 | 01/07/03 | 21 |
| L590* | Staindale Beck | 11.1 $km^2$ | SE 85930 89451 | 18/02/20 | 2.5 |

The geographic characteristics of the catchments used for flow frequency analysis are shown in Fig. S1 and summarised here. The catchment draining into L2725 has 62 km of river network, mostly comprised of first-order streams after the Strahler (1957) stream order notation and has an elevation range of 35–276 mAOD (metres Above Ordnance Datum). It is dominated by coniferous woodland (58%) and improved grassland (20%). The study catchment draining into L590 is a sub-catchment of L2725, with 20.3 km of river network, an elevation range of 105–276 mAOD, and is also dominated by coniferous woodland (69%) and improved grassland (15%). The adjacent catchment to the east, F25110, has 22.6 km of river network and is predominantly improved grassland (42%) and heathers (33%) with an elevation range of 73–289 mAOD.

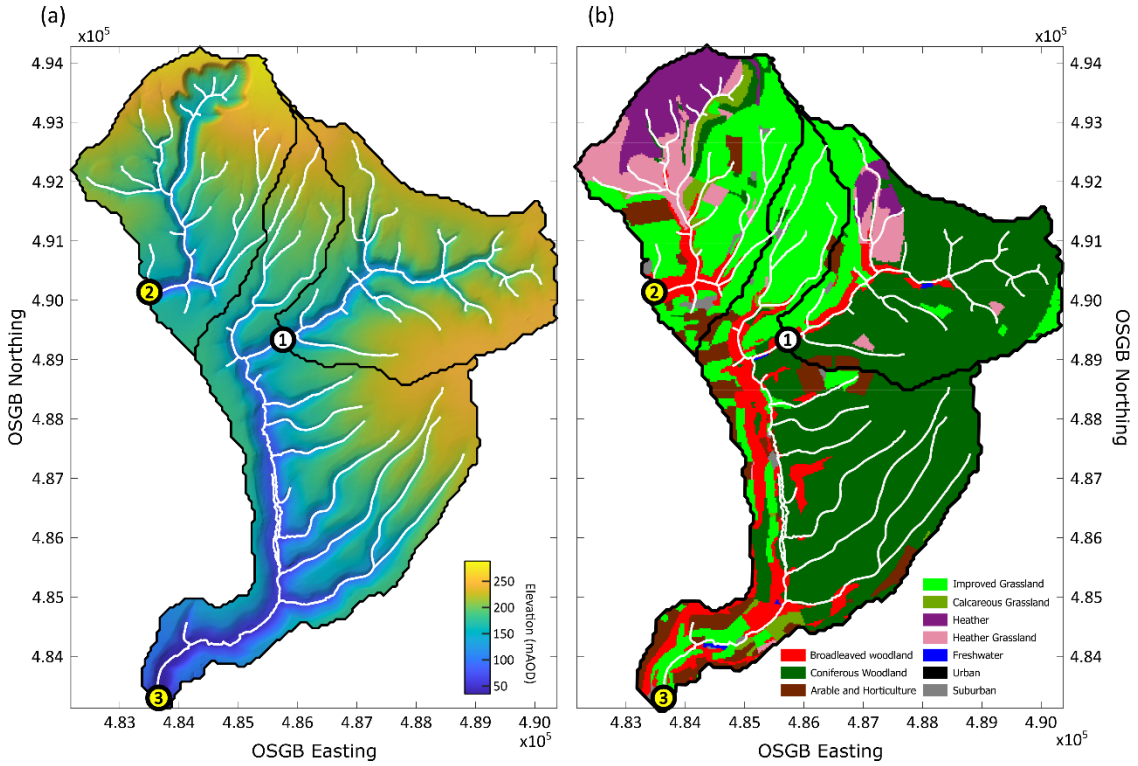


*Fig. S1: a) OS Terrain 5 elevation (Ordnance Survey, 2020) and stream network (white) of the study area delineated by catchments including the study area (1), the area upstream of F25110 (2) and upstream of L2725 (3). b) 25 m Land Cover Map for the area of interest (Morton et al., 2021).*

## *Results*

Annual maxima for water years were extracted from the full time series for analysis. Extreme values for F25110 that were greater than the confidence limit for the site (0.4 m) were removed except for two readings (0.4820 m [2023] and 0.4090 m [2012]) to attempt to constrain substantial flow events. The data was fit to the Generalized Extreme Value Distribution in MATLAB with a 95% confidence interval to produce a rating curve (Fig. S2). The majority of annual maximum flows and levels—plotted using both Weibull (1939) and Gringorten (1963) plotting distribution methods—were within the 95% confidence limits.

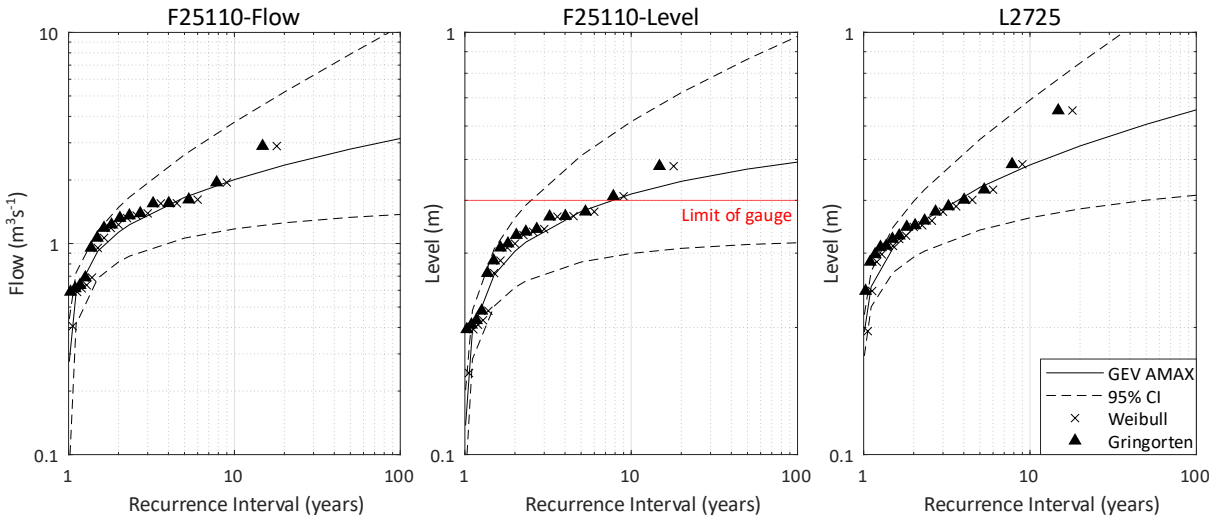


*Fig. S2: Graphical frequency analysis for Environment Agency data fit to the Generalized Extreme Value Distribution. Also shown are the Weibull and Gringorten plotting positions.*

To directly compare the level gauge data, the full dataset was median normalised (Fig. S3a). There is good agreement for 90% of the flow time, however F25110-level is elevated for the 0–10% of flows, suggesting a flashier response than L2725. For comparison to the most upstream levelogger installed at site 2, the full dataset was sampled to the monitoring period (18/02/2020–11/08/2022), and the logger retimed to match the gauges (15-minute resolution). The logger installed as part of this study most closely matches that of L2725 but also shows a similar agreement to F25110-level for 90% of flows (Fig. S3b). Elevated values for F25110-level and L2725 at exceedances > 0.85 suggest greater storage in the catchments, which was expected as it is a larger catchment fed by other streams, many of which are supported by a chalk aquifer. Elevated values for F25110-level and L2725 at exceedances <0.5 suggest that there are more frequent mid- to upper-range events, which is surprising given their proximity, but may be explained by differences in dominant land cover (forest vs grassland) and basin morphometry. Elevated values at the 0-0.1 exceedances suggest that F25110-level and L2725 are flashier than the study site.

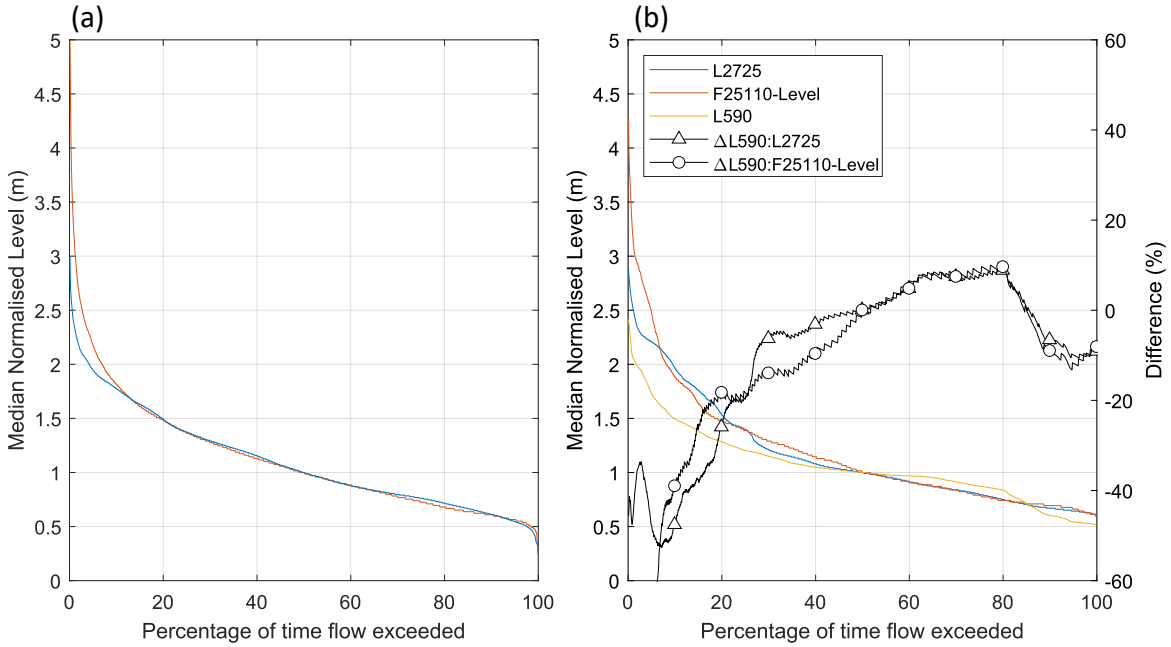


*Fig. S3: Median normalised level for the period of record for Environment Agency gauges L2725 and F25110 (a) and for the study period (b). The most upstream site level logger (L590) is also shown, with the percentage difference when compared to L2725 and F25110-level.*

The subsampled hydrographs were cross correlated to L590 whilst varying the lag period to assess their temporal agreement. L2725 had a maximum correlation of 0.942 with a lag range of –15–45 minutes whilst F25110-level had a slightly higher correlation with a maximum of 0.962 when the lag was 30–60 minutes.

Overall, there is a good agreement between the hydrographs for the different logger sites. Therefore, in lieu of any other flow data, the flow frequency analysis from L2725 and F25110 was applied to L590 to estimate the rarity of events during the monitoring period as discussed in the main text of the manuscript.

**S2. Topography and bathymetric data processing**

*Data Processing*

Referenced point clouds were manually cropped to the area of interest. Vegetation was removed where possible to create a bare-ground point cloud for change analysis using the cloth simulation filter (CSF) plugin in CloudCompare (Zhang et al., 2016). The LD and any remaining channel overhanging vegetation were removed manually by adjusting the viewpoint of the point cloud and using the segment tool in CloudCompare to visually identify vegetation based on prominence from the surrounding point cloud and site knowledge.

Finally, the processed point cloud was gridded in Surfer® 8. To generate the grid, minimum and maximum $x$ and $y$ coordinates were predefined to ensure an identical grid for all survey dates, with the same grid resolution, retaining the minimum elevation point in each cell to decrease the likelihood of including low-lying vegetation. A resolution of 0.1 m was chosen as this is coarser than the TLS and TS recorded accuracies (TOPCON, 2017a, 2017b) and the horizontal georeferencing errors. The grid was generated using triangulation with linear interpolation which is an exact interpolator that preserves raw data points, as recommended by Schwendel et al. (2012).

*Error quantification*

TLS error was quantified through calculating tie point accuracy by comparing the TS coordinate data to the TLS tie point coordinates for each survey position. Residual distance (i.e., the distance between the measured point and the interpolated point in 3D space; the raw elevation survey error) between tie points was calculated during registration for each dimension (i.e., $x$, $y$ and $z$). Across all point clouds, the georeferencing error was greater than internal registration error, as such the georeferencing error is used to assess the total error across an individual cloud. Horizontal error is typically within the same order of magnitude of the vertical error but has little influence on vertical surface differences in most fluvial environments (Wheaton et al., 2010). Therefore, to assess registration quality, only the residuals in the $z$ dimension were considered by calculating the root mean square error (RMSE) as a measure of goodness of fit of the DEM to the surveyed points, commonly used to evaluate map accuracy (Fisher and Tate, 2006). To provide a more complete overview of error beyond RMSE, the mean error (ME), the standard deviation of the mean error (SD), and mean absolute error (MAE) were also calculated (Fisher and Tate, 2006; Schwendel et al., 2012).

All deviations shown in Table S2 are very low, generally sub-centimetre for both TS and TLS data. ME results are weakly positively biased, indicating that elevations were slightly overestimated during registration. SD and RMSE have a similar order of magnitude and are also consistent between surveys, for both TS and TLS, therefore these data are appropriate for further analysis (Schwendel et al., 2012). RMSE, SD and MAE for the TLS registration points are larger than those reported for the TS sample points, likely due to the influence of number of observations (five independent check points vs averages of 71 [site 1] and 110 [site 2] for TS). Nevertheless, all vertical errors for TS are <0.013 m, indicating a high level of accuracy of the gridded DEM representing the bathymetric topography. All TLS vertical errors are <0.026 m, except for April and November of 2021 for LD1 which have a maximum error of 0.043 m and 0.034 m, respectively.

*Table S2: Error metrics for survey residuals. All values are reported in metres, the maximum error for each metric for each site is highlighted in bold.*

| | | LD1 | | | | LD2 | | | |
|---|---|---|---|---|---|---|---|---|---|
| | | RMSE | ME | SD | MAE | RMSE | ME | SD | MAE |
| TS | 15/07/2019 | 0.006 | 0.006 | <0.001 | 0.003 | 0.005 | 0.004 | -0.001 | 0.003 |
| | 28/01/2020 | 0.005 | 0.005 | <0.001 | 0.003 | 0.007 | 0.007 | -0.001 | 0.004 |
| | 27/09/2020 | - | - | - | - | 0.010 | 0.010 | -0.001 | 0.004 |
| | 07/01/2021 | 0.007 | 0.007 | <0.001 | 0.004 | 0.007 | 0.007 | -0.001 | 0.004 |
| | 26/01/2021 | - | - | - | - | **0.013** | **0.013** | **-0.002** | **0.009** |
| | 07/04/2021 | **0.009** | **0.009** | <0.001 | **0.005** | 0.008 | 0.008 | -0.001 | 0.005 |
| | 20/08/2021 | 0.006 | 0.006 | <0.001 | 0.004 | 0.008 | 0.008 | <0.001 | 0.005 |
| | 30/11/2021 | 0.008 | 0.008 | **-0.002** | 0.004 | 0.008 | 0.008 | **-0.002** | 0.005 |
| | 11/02/2022 | - | - | - | - | 0.006 | 0.006 | <0.001 | 0.005 |
| | 14/04/2022 | 0.006 | 0.006 | <0.001 | 0.004 | 0.009 | 0.009 | <0.001 | 0.004 |
| | 11/08/2022 | - | - | - | - | 0.007 | 0.007 | <0.001 | 0.005 |
| TLS | 15/07/2019 | 0.006 | <0.001 | 0.006 | 0.004 | 0.021 | <0.001 | 0.024 | 0.018 |
| | 28/01/2020 | 0.004 | <0.001 | 0.005 | 0.004 | **0.026** | <0.001 | **0.029** | **0.024** |
| | 27/09/2020 | 0.009 | 0.001 | 0.010 | 0.008 | 0.014 | **-0.003** | 0.016 | 0.012 |
| | 07/01/2021 | - | - | - | - | 0.025 | 0.001 | 0.028 | 0.023 |
| | 26/01/2021 | 0.011 | -0.001 | 0.013 | 0.010 | 0.010 | <0.001 | 0.011 | 0.009 |
| | 07/04/2021 | **0.043** | **0.002** | **0.050** | **0.039** | 0.007 | 0.001 | 0.007 | 0.006 |
| | 20/08/2021 | 0.008 | <0.001 | 0.009 | 0.007 | 0.004 | 0.001 | 0.005 | 0.003 |
| | 30/11/2021 | 0.034 | <0.001 | 0.038 | 0.026 | 0.017 | 0.001 | 0.019 | 0.016 |
| | 11/02/2022 | 0.003 | <0.001 | 0.004 | 0.003 | 0.004 | <0.001 | 0.005 | 0.004 |
| | 14/04/2022 | 0.006 | <0.001 | 0.006 | 0.004 | 0.021 | <0.001 | 0.024 | 0.018 |
| | 11/08/2022 | 0.004 | <0.001 | 0.005 | 0.004 | **0.026** | <0.001 | **0.029** | **0.024** |

**S3. References**


Fisher, P.F., Tate, N.J., 2006. Causes and consequences of error in digital elevation models. Prog. Phys. Geogr. Earth Environ. 30, 467–489. https://doi.org/10.1191/0309133306pp492ra

Gringorten, I.I., 1963. A plotting rule for extreme probability paper. J. Geophys. Res. 1896-1977 68, 813–814. https://doi.org/10.1029/JZ068i003p00813

Hydrology NE Environment Agency, 2024. Stage data from gauging stations L2725 and F25110, licensed under the Open Government Licence v3.0 nationalarchives.gov.uk.

Morton, R.D., Marston, C.G., O'Neil, A.W., Rowland, C.S., 2021. Land Cover Map 2020 (25m rasterised land parcels, GB).

Ordnance Survey, 2020. OS Terrain 5 DTM [ASC geospatial data], Scale 1:20000, Tile(s): Dalby Forest, Updated: April 2020.

Schwendel, A.C., Fuller, I.C., Death, R.G., 2012. Assessing DEM interpolation methods for effective representation of upland stream morphology for rapid appraisal of bed stability. River Res. Appl. 28, 567–584. https://doi.org/10.1002/rra.1475

Strahler, A.N., 1957. Quantitative analysis of watershed geomorphology. Eos Trans. Am. Geophys. Union 38, 913–920.

TOPCON, 2017a. GLS-2000 Data Sheet.

TOPCON, 2017b. OS Series Data Sheet.

Weibull, W., 1939. A statistical theory of strength of materials. IVB-Handl.

Wheaton, J.M., Brasington, J., Darby, S.E., Sear, D.A., 2010. Accounting for uncertainty in DEMs from repeat topographic surveys: improved sediment budgets. Earth Surf. Process. Landf. 136–156. https://doi.org/10.1002/esp.1886

Zhang, W., Qi, J., Wan, P., Wang, H., Xie, D., Wang, X., Yan, G., 2016. An Easy-to-Use Airborne LiDAR Data Filtering Method Based on Cloth Simulation. Remote Sens. 8. https://doi.org/10.3390/rs8060501